ANNALS OF MEDICINE
2024, VOL. 56, NO. 1, 2408463
https://doi.org/10.1080/07853890.2024.2408463

RESEARCH ARTICLE

OPEN ACCESS Check for updates

Analysis of the implication of steroid 5 alpha-reductase 3 on prognosis and immune microenvironment in Liver Hepatocellular Carcinoma

Yuming Lu[a‡], Ziwei Liu[b‡], Yu Zheng[c‡], Xuesong Liu[d], XiaoQin Liu[c], Nanguan Chen[e], Kai Mao[c] and Weida Lin[c]

[a]Department of Biostatistics, College of Science, City University of Hong Kong, Hong Kong, China; [b]School of Nursing, Guangzhou Medical University, Guangzhou, Guangdong, China; [c]Department of Hepatobiliary Pancreatic Surgery, ShenShan Medical Center, Memorial Hospital of Sun Yat-Sen University, Shanwei, Guangdong, China; [d]Department of Immunology, BinZhou Medical University, Binzhou, Shandong, China; [e]Luoding Hospital of Traditional Chinese Medicine, Luoding, Guangdong, China

ABSTRACT

Introduction: This study combined the bioinformatics and *in vitro* experiment-related technologies to analyze the impact of steroid 5 alpha-reductase 3 (SRD5A3) on the prognosis and immune microenvironment of Liver Hepatocellular Carcinoma (LIHC).

Method: Gene expression and clinical data were obtained from public databases. The prognosis was evaluated using survival, multifactor Cox, enrichment, and mutation analyses. This was then verified through *in vitro* experiments.

Results: The expression level of *SRD5A3* in LIHC tissues was significantly higher than that in the adjacent tissues. Kaplan–Meier survival analysis showed that high *SRD5A3* expression was associated with poor overall survival (OS) and short progression-free survival in patients with LIHC. Multivariate Cox regression analysis revealed that positive *SRD5A3* expression was an independent risk factor for OS in patients with LIHC. Expression of *SRD5A3* was negatively correlated with immune cell infiltration of CD4+ T, CD8+ T, and B cells. GO and KEGG enrichment analyses showed that *SRD5A3* was significantly enriched in signaling- and tumor metastasis-related pathways. Nomogram and calibration curve showed that the predicted performance of the model was consistent with the actual results. *In vitro* results confirmed that *SRD5A3* knockdown inhibited the migration, invasion, and proliferation of LIHC cells.

Conclusions: *SRD5A3* is actively expressed in LIHC, and positive expression of *SRD5A3* is an independent risk factor for different prognoses in patients with LIHC. *SRD5A3* can promote the proliferation, migration, and invasion of liver cancer cells and is related to short immune infiltration in patients with LIHC.

KEY MESSAGES

1. High *SRD5A3* expression is significantly associated with poor prognosis in patients with LIHC and may help assess tumor progression.
2. Highly expressed *SRD5A3* promotes migration, invasion, and proliferation of liver cancer cells.
3. *SRD5A3* expression is related to the degree of tumor immune cell infiltration.

ARTICLE HISTORY
Received 14 October 2023
Revised 2 May 2024
Accepted 2 May 2024

KEYWORDS
Steroid 5 alpha-reductase 3; Liver Hepatocellular Carcinoma; single cell sequencing; prognosis; immunotherapy

1. Introduction

Liver Hepatocellular Carcinoma (LIHC) is the most common cause of cancer-related deaths worldwide [1,2]. Most patients are diagnosed with LIHC at an advanced stage, and early detection and treatment can greatly improve survival rate of the patient [3]. Therefore, identifying new biomarkers and further exploring their possible pathogenesis are crucial for the diagnosis and treatment of LIHC.

Treatment methods for liver cancer include surgical resection, radiotherapy, chemotherapy, interventional embolization, and targeted therapy. Surgical treatment for early stage liver cancer typically has a curative effect [4]. Despite this, most patients miss the

CONTACT Kai Mao mkz31@163.com; Weida Lin lwd7189@163.com Department of Hepatobiliary Pancreatic Surgery, ShenShan Medical Center, Memorial Hospital of Sun Yat-Sen University, Shanwei 516621, China
‡These authors contributed equally to this work.

Supplemental data for this article can be accessed online at https://doi.org/10.1080/07853890.2024.2408463.

optimum opportunity for treatment because they are already in intermediate and advanced stages when they seek treatment. In addition, some patients experience tumor recurrence after undergoing treatment. Tumor markers are mostly found in malignant tumor cells. They are markers produced by tumor cells or the host immune stimulation of tumor responses [5]. They can accurately reflect the occurrence and development of tumors and allow early detection and effective treatment of tumors. Therefore, there is an urgent need for in-depth research into liver cancer, including its pathogenesis and therapeutic targets [6].

The tumor microenvironment (TME) includes tumors, immune cells, and stromal components, which play important roles in tumor growth and are closely related to tumor subtypes and grades [7]. Research has shown that inhibiting immune-related genes in the TME can directly slow down tumor growth. Increased expression of immune-related genes has been detected in patients with early stage liver cancer; however, no conspicuous changes have been detected in most patients. Therefore, the expression of TME-related genes is closely related to components such as immune responses and immune cells in tumors [8]. Further research on RME-related genes of liver cancer will help develop targeted drugs and the clinical treatment of LIHC.

Steroid 5 alpha-reductase 3 (SRD5A3) is an enzyme in the steroid 5 alpha-reductase family that plays important roles such as participating in bile acid biosynthesis. However, SRD5A3 mainly produces steroid hormones that regulate male sexual development [9]. It is an important molecule for glycosylation and steroid hormone formation. SRD5A3 proffers reducing hydrogen *via* NADPH to reduce steroid compounds. Moreover, SRD5A3 is involved in N-glycosylation, and mutations in the SRD5A3 gene can lead to congenital glycosylation disorders. Studies have shown that mutations in SRD5A3 can promote the occurrence of benign prostatic hyperplasia and prostate cancer by dysregulating androgen metabolism [10]. In addition, SRD5A3 is positively expressed in breast cancer, endometrial cancer, and human fetal liver [11–13]. These results warrant further research on SRD5A3 expression in LIHC.

This study used bioinformatics analysis and *in vitro* tumor metastasis-related experiments to analyze whether the expression of SRD5A3 in liver cancer undergoes abnormal changes and to explore the regulatory role of abnormal SRD5A3 expression in liver cancer metastasis, providing an insight into clinical immunotherapy for patients with LIHC.

2. Materials and methods

2.1. Data collection and analysis

Gene expression and clinical data for GSE125449 were obtained from the Tumor Immune Single-cell Hub 2 (TISCH2) database (http://tisch2.compgenomics.org/) [14]. The Cancer Genome Atlas (TCGA) database (https://cancergenome.nih.gov/) and Gene Expression Omnibus (GEO; https://www.ncbi.nlm.nih.gov/geo/) were used to analyze the expression of SRD5A3 in various cancers and its relationship with tumor progression [15,16]. Kaplan–Meier curves were drafted to resolve the relationship between *SRD5A3* expression in patients with LIHC and overall survival (OS) and progression-free survival (PFS). Independent prognostic factors were analyzed using univariate and multifactorial Cox analyses. A nomogram was constructed by combining the age, stage, and risk score, and a calibration curve was constructed to evaluate the relationship between *SRD5A3* expression and patient survival. Finally, Gene Ontology (GO) and Kyoto Encyclopedia of Genes and Genomes (KEGG) enrichment of related genes were performed to analyze the regulatory pathways of *SRD5A3* [17,18].

2.2. Immune microenvironment infiltration analysis

The Tumor IMmune Estimation Resource (TIMER) database was used to calculate immune cell infiltration in each sample [19], and the correlation between immune target genes and SRD5A3 expression levels was analyzed. Finally, SRD5A3-related immunomodulators were predicted using the STRING database (https://cn.string-db.org) and enrichment analysis [20].

2.3. Immunohistochemistry

The experiment collected surgical specimens from 15 patients with liver cancer from the ShenShan Medical Center, Memorial Hospital of Sun Yat-Sen University, and all patients gave informed consent. This study was conducted under the approval of the Ethics Committee of the Shen Shan Medical Center, Memorial Hospital of Sun Yat-Sen University in strict accordance with the Declaration of Helsinki (Approval No:2024-SSKY-198-01). No animal studies, human studies in this manuscript. I confirm that all the research meets ethical guidelines and adheres to the legal requirements of the study country. All patients were informed prior to use of patient specimen and signed written informed consents.

The cancer tissue and normal tissue were treated and sliced. The SRD5A3 antibody was used for staining. The images were taken under the microscope and analyzed.

2.4. Cell culture and transfection

The cells were cultured in high-glucose DMEM containing 10% fetal bovine serum (FBS) in a constant-temperature incubator. When the cell density reached 60–70%, siRNAs were transfected into HepG2 and SNU387 cells, and categorized into si-NC (control group) and si-SRD5A3 (experimental group). Follow-up experiments were performed after successful transfection.

2.5. Flow cytometry

HepG2 and SNU387 control and experimental group cells were seeded onto a plate at a density of 4×105 cells/well and incubated for 24 h. After treatment, flow cytometry was used to detect cell apoptosis, according to the instructions of the apoptosis kit.

2.6. Transwell experiment

For cell invasion experiments, 50 µL Matrigel was evenly spread into the upper chamber of the Transwell chamber in advance. Forty-eight hours after transfection, the cells were resuspended in serum-free medium and transplanted into the upper chamber. Fetal calf serum was added to the lower chamber. The cells were then placed in a cell culture incubator, incubated for 24 h, and fixed with crystal violet for 1 h. Finally, images were captured under an inverted microscope, and the percentage of cell migration was statistically analyzed. The cell migration experiment did not require the laying of Matrigel, and the other steps were the same as those used in the cell invasion experiment.

2.7. Western blot

After the cultured cell L-02, HepG2 and SNU387 were cracked with homogenate buffer, the obtained sample was subjected to SDS-PAGE by conventional method. Subsequently, the protein is semi-dry transferred to the membrane. After the end of the transfer, the tested membrane strips were taken for western blot experiment. When adding sealer, be careful to avoid non-specific reactions. After washing, the first antibody and the second antibody were added for reaction. Finally, the film is exposed in a darkroom, and the obtained signal strips are scanned to calculate their integral optical density.

2.8. ELISA experiment

HepG2 normal and knockdown cell lines were cultured with human CD8T cells. After a certain time, the cells were collected by centrifugation and appropriate lysate was added. After sufficient cracking, the supernatant sample was taken and diluted appropriately. This was followed by routine assays using IFN-γ, CD27, and CD28 ELISA kits to determine protein concentrations.

2.9. Statistical analysis

The experimental results were statistically analyzed using GraphPad Prism software (version 8.0), and the count results between the experimental and control groups were analyzed and evaluated using an independent sample t-test or one-way analysis of variance. Statistically significant difference was set at $p < 0.05$.

3. Results

3.1. Detection of SRD5A3 expression in LIHC using single-cell sequencing

First, based on the TISCH2 database, the cell types and distribution of patients with LIHC in the GSE125449 dataset were analyzed. In addition to malignant tumors, other immune microenvironment cells, such as B cells and CD8+ T cells, were also included (Figure 1A). Using the detailed cell-type annotation of SRD5A3 at single-cell level, the expression of SRD5A3 in LIHC was investigated, and SRD5A3 was found to be expressed in tumor cells and in cells related to the TME (Figure 1B,C).

3.2. SRD5A3 is upregulated and associated with negative prognosis in LIHC

Regarding the pan-cancer expression level, SRD5A3 was highly expressed in various malignant tumors ($p < 0.05$; Figure 2A). The expression level of SRD5A3 in liver cancer was significantly higher than that in adjacent para-cancerous tissues in both unpaired and paired samples ($p < 0.001$; Figure 2B,C). According to the median SRD5A3 expression, patients with liver cancer were divided into high ($n = 185$) and low ($n = 185$) SRD5A3 expression groups. As shown in Figure 2D, compared to the low SRD5A3 expression group, the OS rate of patients in the high SRD5A3 expression group was worse ($p < 0.001$). Simultaneously, the PFS of patients in the high SRD5A3 expression group was also poor ($p < 0.001$; Figure 2E).

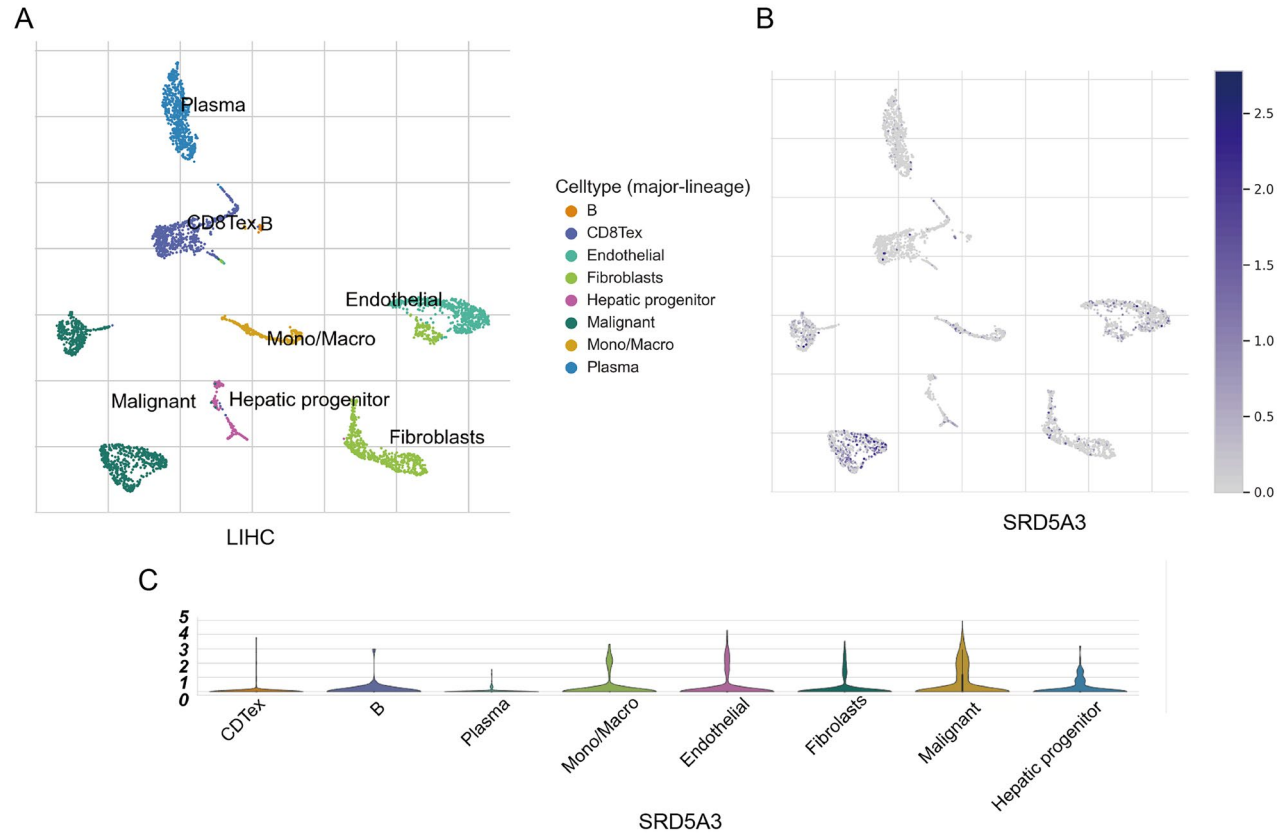

Figure 1. Detection of SRD5A3 expression in Liver Hepatocellular Carcinoma by single-cell sequencing. (A) TISCH2 database of GSE125449 LIHC single-cell datase. (B,C) Expression of SRD5A3 gene in GSE125449 data.

3.3. Correlation analysis of SRD5A3 expression and clinical features in LIHC

Stratified analysis of all patients with LIHC showed that compared to low SRD5A3 expression, the prognosis of LIHC patients with high SRD5A3 expression was significantly worse in the female subgroup, stage I, stage II, T1, and T2 ($p < 0.05$; Figure 3A–F). As shown in Figure 3G, detailed clinical characteristics of each patient are included. Univariate and multivariate Cox proportional hazards regression analyses revealed that the expression level of SRD5A3 was an independent risk factor for the OS of patients with LIHC (Figure 4A,B). According to the relevant clinical variables in the multivariate Cox regression analysis, a nomogram based on OS-independent factors was generated to predict the 1-, 3-, and 5-year prognoses of patients. In the nomogram, the greater the total number of points, the worse was the prognosis (Figure 4C). The model had a moderate predictive accuracy for OS in patients with LIHC (Figure 4D,E).

3.4. Enrichment analysis of SRD5A3 in LIHC

We compared the expression of relevant differential genes in the positive and negative expression groups and performed an enrichment analysis on the differentially expressed genes. GO enrichment analysis showed that the significantly enriched biological processes included biological processes (BP): extracellular matrix organization and extracellular structure organization; cellular components (CC): the apical part of the cell; and molecular function (MF): signaling receptor activator activity (Figure 5A,B). KEGG pathway enrichment analysis showed that the significantly enriched pathways included positive regulation of kinase activity (Figure 5C,D).

3.5. Correlation analysis of SRD5A3 expression level and immune cell infiltration in LIHC

Analysis of *SRD5A3* expression levels in the single cell database is inversely proportional to the number of CD8+ T cells (R=-0.31, $p < 0.01$, Figure 6A). Using the TIMER public database analysis, the reduced infiltration of CD8+ T cells was related to the increased expression of *SRD5A3* (R=-0.153, $p < 0.01$, Figure 6B). Furthermore, the levels of cellular infiltration in various pan-cancer TMEs were assessed (Figure 6C). According to Spearman correlation analysis, the immune infiltration level of effector memory CD8+ T cells (Tem-CD8+T) was inversely correlated with *SRD5A3* expression (R=-0.108,

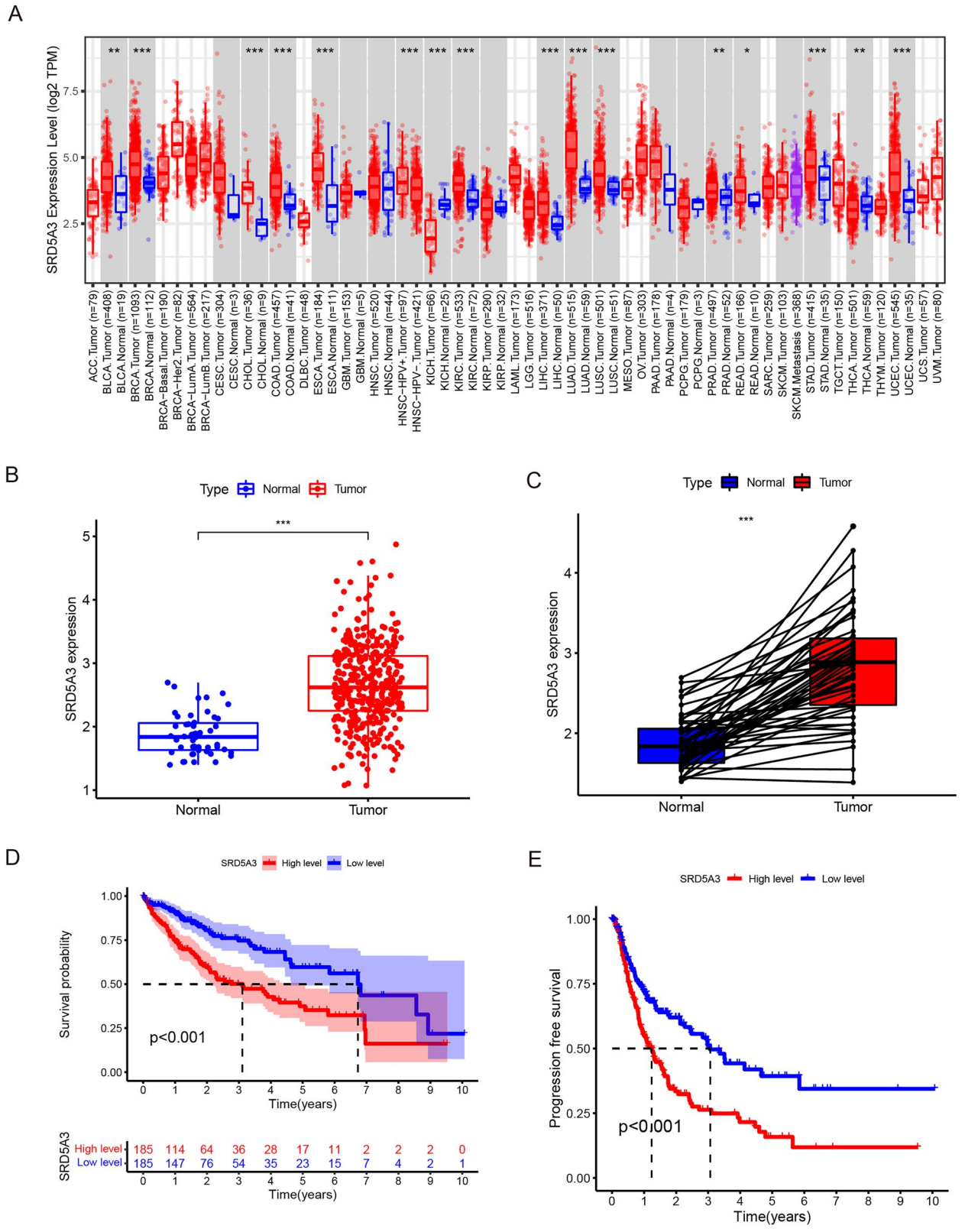

Figure 2. The expression level of SRD5A3 and its correlation with prognosis in LIHC. (A) Expression levels of SRD5A3 in different tumors compared with normal tissues in the databases. (B) Expression levels of SRD5A3 in LIHC and unpaired normal tissues from the databases. (C) Expression of SRD5A3 in LIHC and paired normal tissues in the database. (D) K-M curves of different SRD5A3 expressions in LIHC. (E) PFS survival curve of different SRD5A3 expression in LIHC.

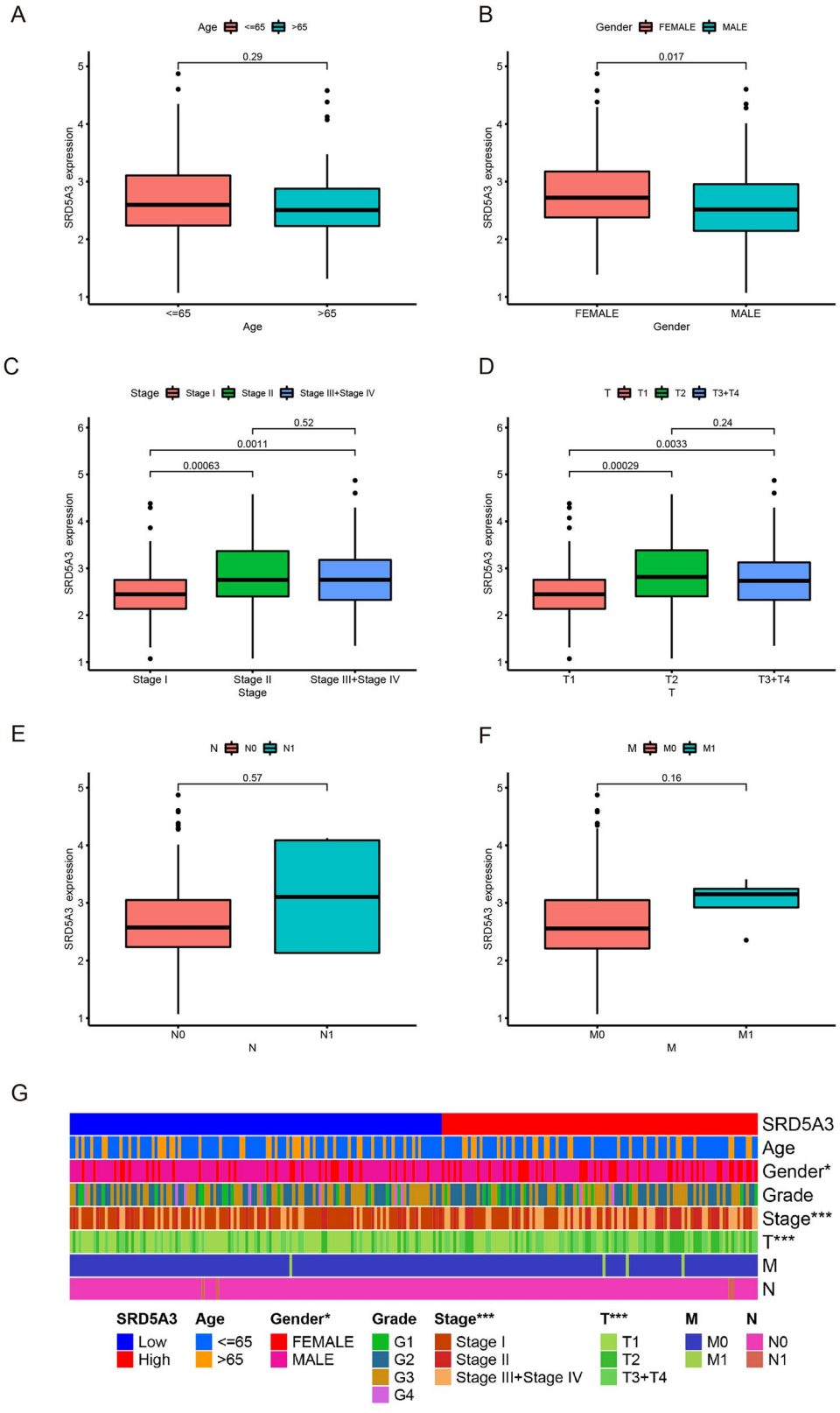

Figure 3. Correlation analysis of SRD5A3 expression and clinical features in LIHC. (A–F) The expression of SRD5A3 in LIHC is distributed among age, gender, and T, N, M, and stage groups. (G) Heat map of the relationship between SRD5A3 expression and age, gender, T, N, M, stage group in each LIHC patient.

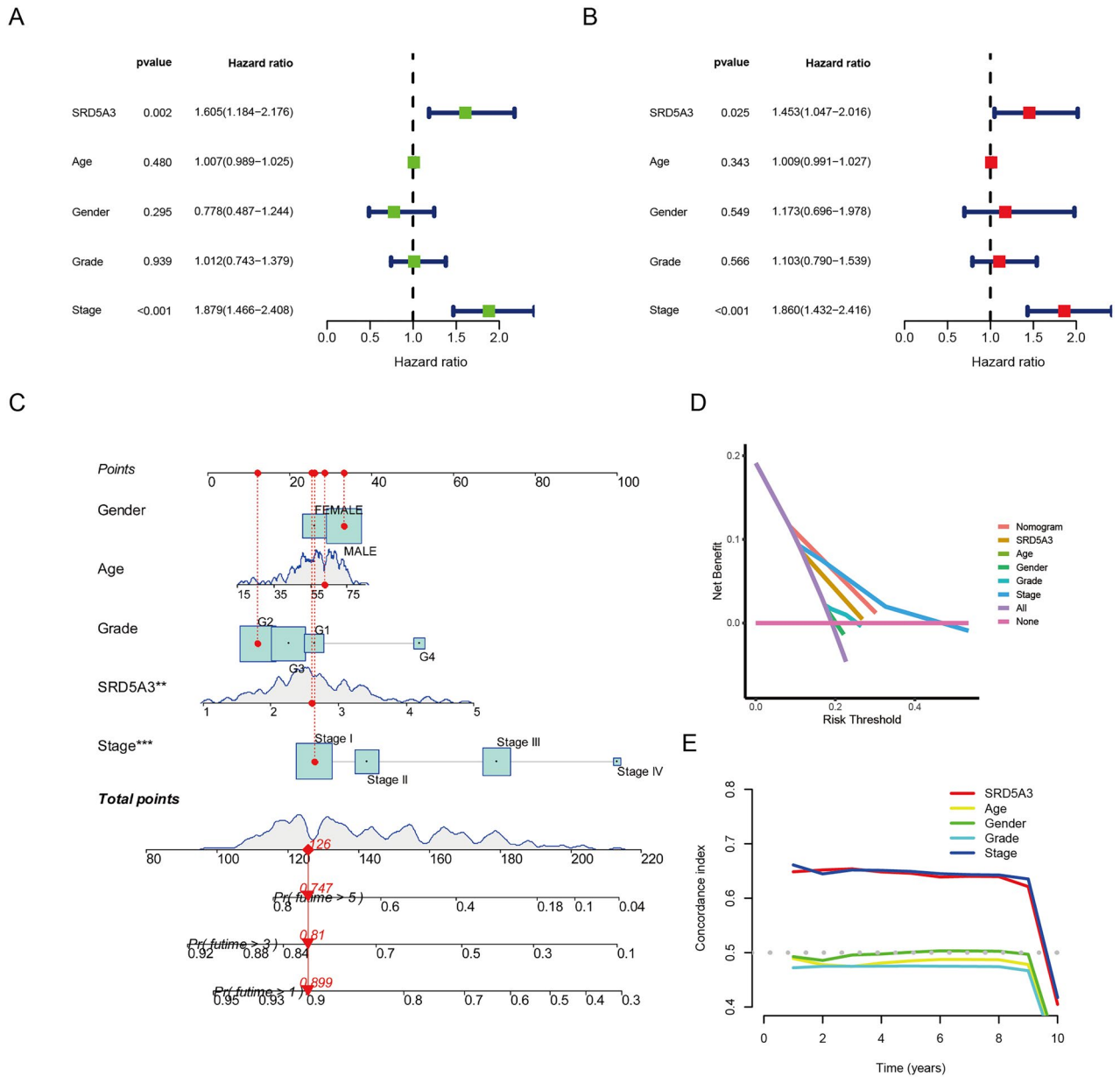

Figure 4. SRD5A3 Expression and clinical features assess the prognosis of LIHC. (A) Univariate Cox analysis Forest plot. (B) Multivariate Cox analysis Forest plot. (C) SRD5A3 expression is combined with age and stage to draw a nomogram, and the 1, 3, and 5-year survival rate can be predicted based on its total score. (D,E) T calibration plots evaluate the accuracy of hybrid models in predicting 1, 3, and 5-year survival and related indices.

$p < 0.05$, Figure 6D). In addition, the higher the expression level of SRD5A3 protein, the lower the infiltration level of activated CD4+ T cells (Act-CD4+T) in the tumor (R=-0.131, $p < 0.05$, Figure 6E), and the fewer activated B cells (Act-B) in the tumor tissue (R=-0.198, $p < 0.001$, Figure 6F).

Correlation analysis between *SRD5A3* expression and various immune checkpoints in LIHC was conducted. We evaluated the pan-cancer distribution of various immune-targeted genes (Figure 7A). The research results found that the expression of IL10RB was positively correlated with the expression of *SRD5A3* ($R = 0.176$, $p < 0.001$, Figure 7B), whereas the expression of BTLA was poorly correlated with the expression of *SRD5A3*. The expression status was negatively correlated (R=-0.173, $p < 0.001$, Figure 7C). Finally, we evaluated the pan-cancer distribution of various immune proteins (Figure 7D). The research results found that the expression of CD27 (R=-0.108, $p < 0.05$, Figure 7E) and CD28 (R=-0.104, $p < 0.05$, Figure 7F) proteins were negatively correlated with that of *SRD5A3*.

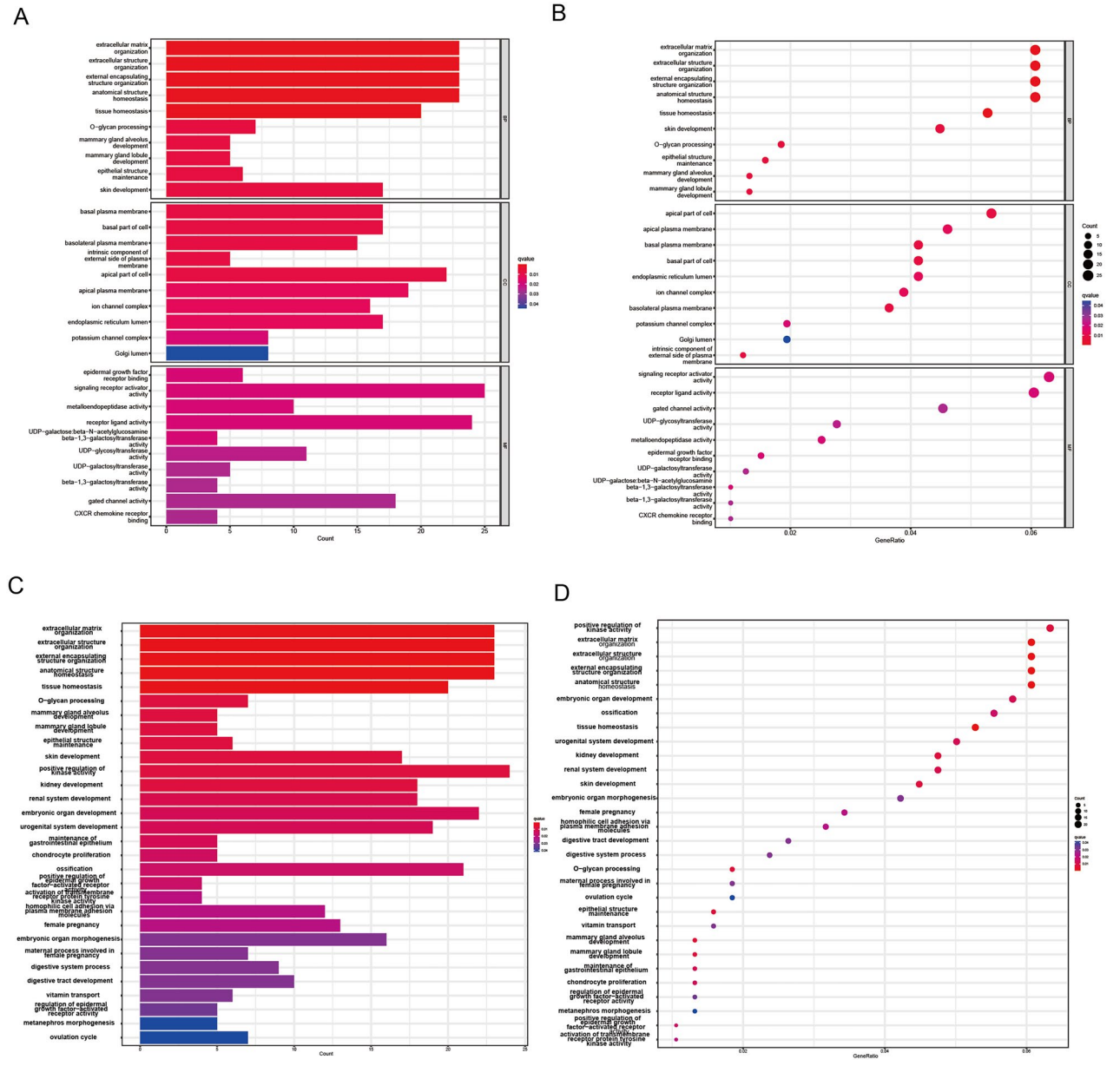

Figure 5. Enrichment analysis of SRD5A3 in LIHC. (A) GO analysis histogram. (B) GO analysis scatter plot. (C) KEGG analysis histogram. (D) KEGG analysis scatter plot.

3.6. Identification and analysis of SRD5A3-associated immunomodulators

The immune checkpoint proteins related to SRD5A3 were analyzed and the expression of IL-10RB, CD27, CD28, BTLA, and SRD5A3 were found to be closely related, which further confirmed the aforementioned results (Figure 8A). The genes of related proteins were then enriched and analyzed. GO enrichment analysis showed that the significantly enriched biological processes included BP: biological regulation, CC: membrane, and MF: protein binding (Figure 8B). KEGG pathway enrichment analysis revealed that the significantly enriched pathways included cytokine–cytokine receptor interactions, intestinal immune networks for IgA production, and cell adhesion molecules (CAMs) (Figure 8C).

3.7. SRD5A3 knock-down inhibits the proliferation and invasion of liver cancer cells, and promotes cell apoptosis

Comparing the cancer tissue and adjacent tissue of 15 liver cancer patients, the expression of *SRD5A3* in cancer tissue was higher than that of normal adjacent tissue ($p < 0.01$, Figure 9A). Knockdown of SRD5A3 in liver cancer cells HepG2 and SNU387 using siRNA. Western

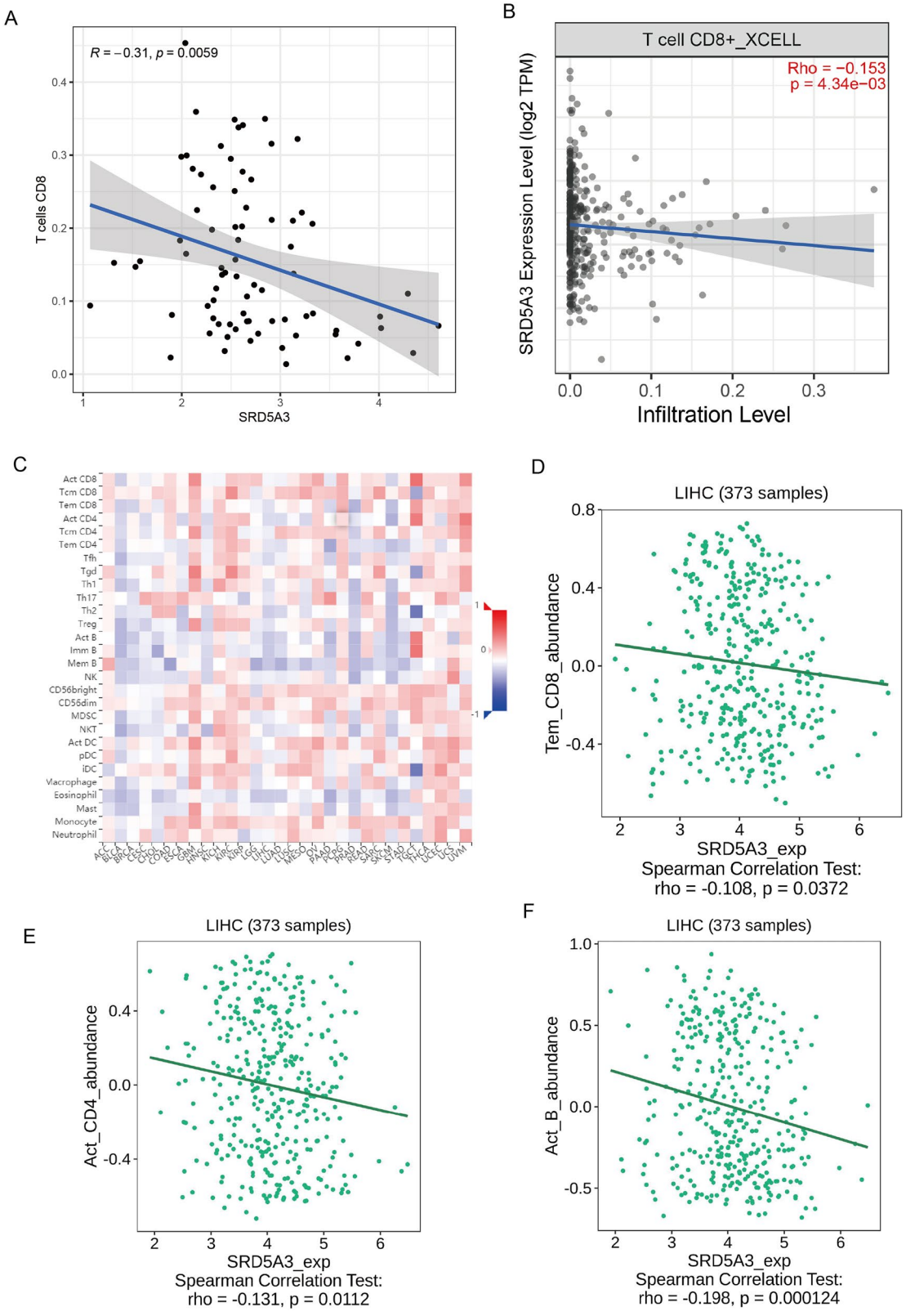

Figure 6. Correlation analysis of SRD5A3 expression level and immune cell infiltration in LIHC. (A,B) The relationship between the expression of CD8 T cells and the expression level of SRD5A3. (C) Heat map of expression levels of different cell types in different cancers. (D,F) Correlation between CD8 T cell, CD4 T cell, B cell expression and SRD5A3 expression levels in LIHC.

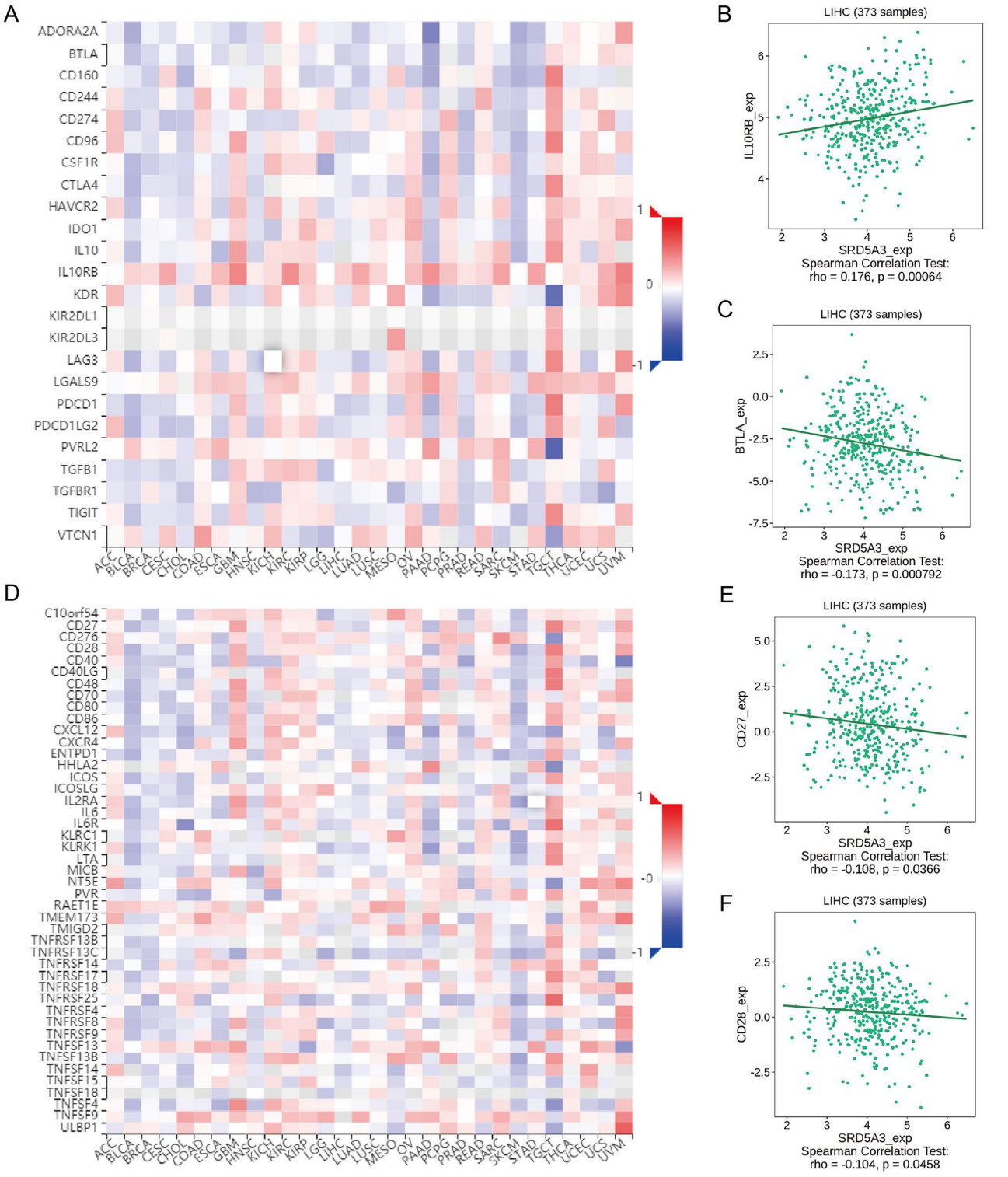

Figure 7. Correlation analysis between the expression of SRD5A3 and various immune checkpoints in LIHC. (A) Heat map of gene expression in different cancers. (B,C) Relationship between IL-10RB, BTLA gene expression and SRD5A3 expression in LIHC. (D) Heat map of protein expression in different cancers. (E,F) Relationship between CD28, CD27 protein expression and SRD5A3 expression in LIHC.

blot experiments showed that these two cells showed relatively high *SRD5A3* expression, while the normal liver cell line L-02 and the knockdown liver cancer cell line had low *SRD5A3* expression (Figure 9B). See Supplementary Material for original strips. The transfected cells were cultured, and flow cytometry was used to detect the proportion of apoptotic cells. The results showed that the proportion of apoptotic cells

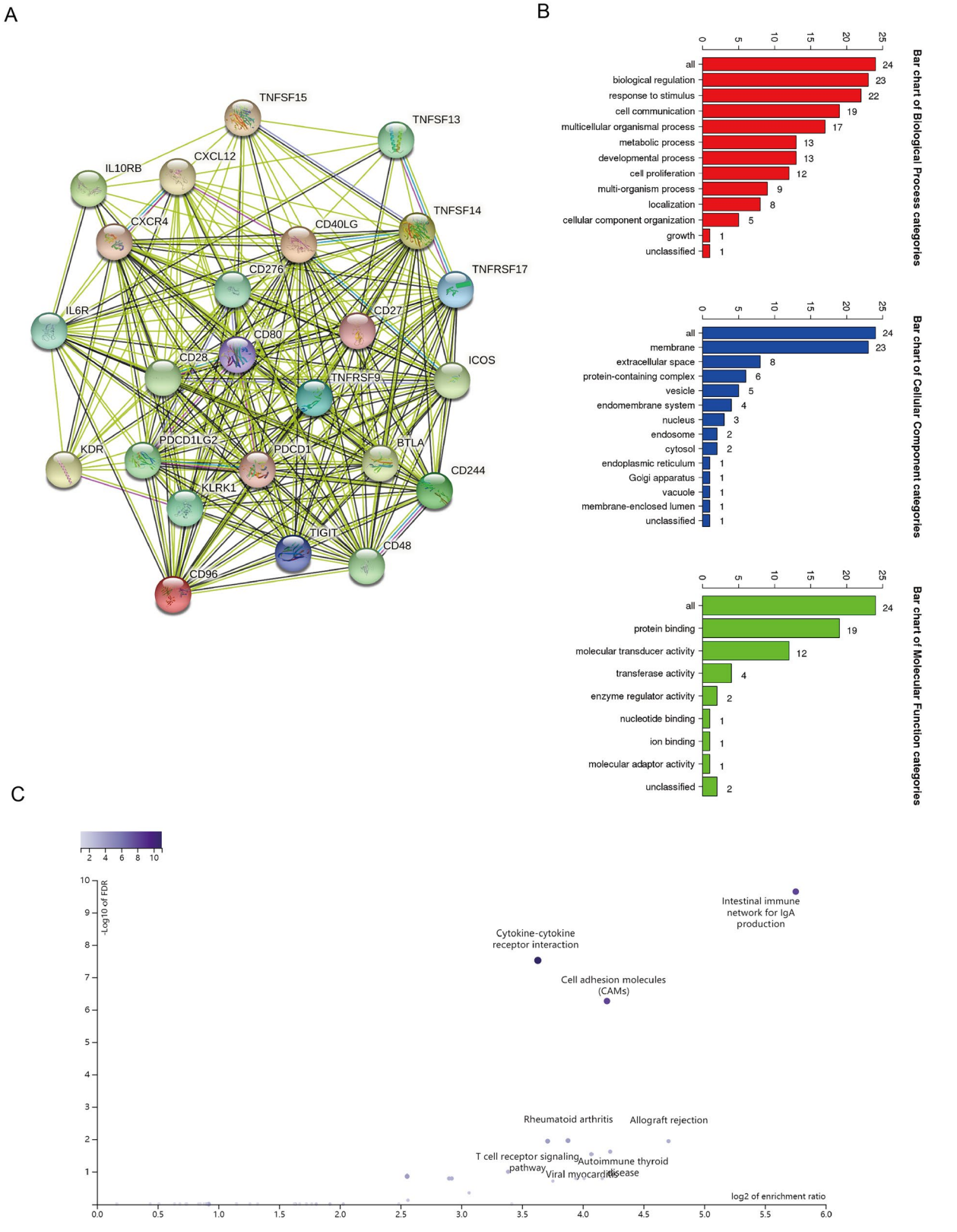

Figure 8. Identification and analysis of immunomodulators associated with the SRD5A3. (A) Network diagram of immune regulatory genes related to SRD5A3. (B) Go enrichment analysis diagram of immune regulatory genes related to SRD5A3. (C) KEGG enrichment analysis diagram of immune regulatory genes related to SRD5A3.

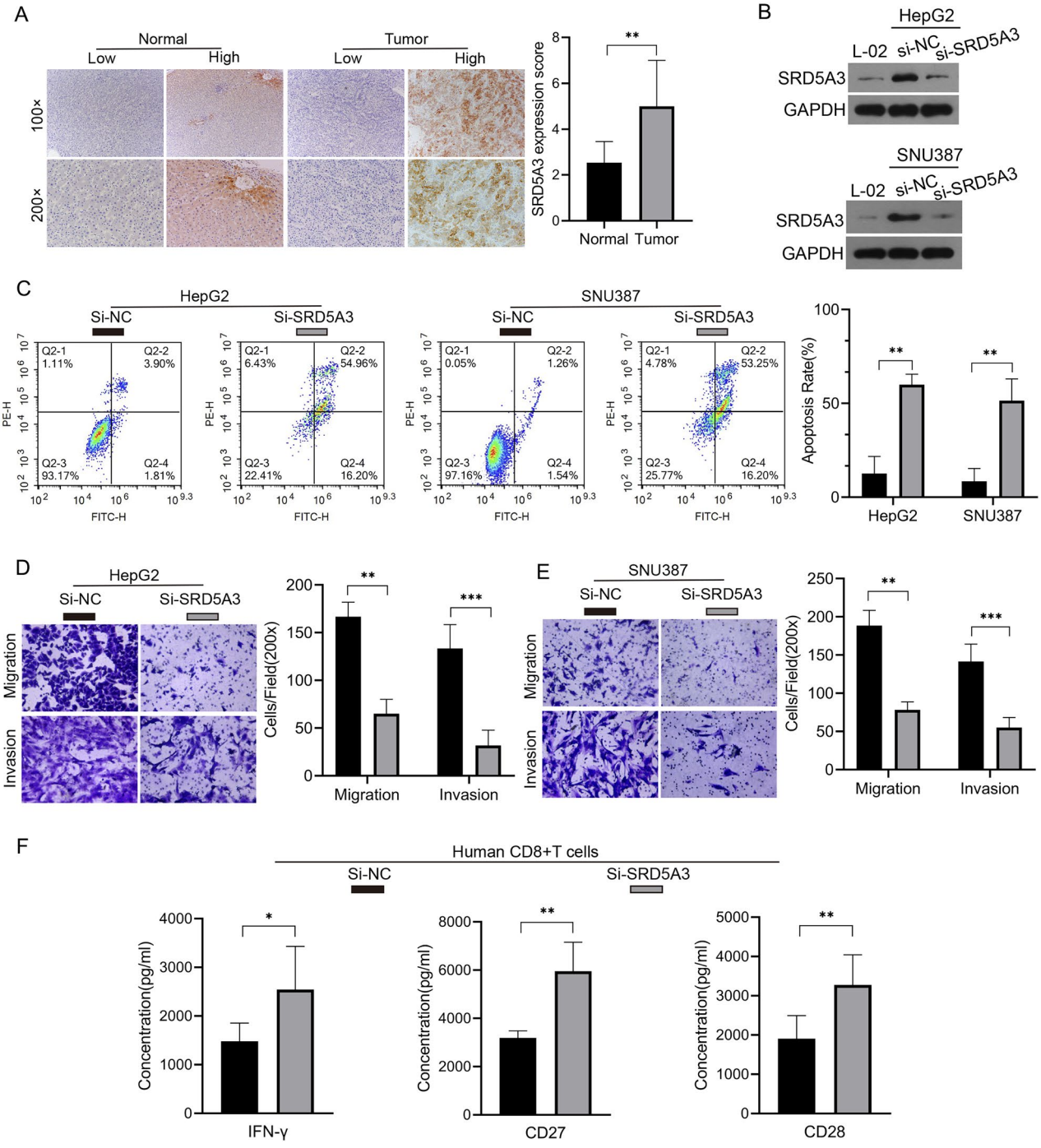

Figure 9. Knockdown of SRD5A3 can inhibit the proliferation and invasion of liver cancer cells. (A) Expression of SRD5A3 in cancer tissues and Para-cancerous tissues in patients with liver cancer. (B) Expression of SRD5A3 in liver cell line L-02, liver cancer cell lines HepG2, SNU387 and knockdown cell lines. (C) Flow cytometry detection and apoptosis ratio of transfected HepG2 and SNU387 cells. (D,E) Migration and invasion of HepG2 and SNU387 cells with SRD5A3 knockdown assessed by Transwell assay (x200). (F) Expression of IFN-γ, CD27, and CD28 after HepG2 cells in Si-NC and si-SRD5A3 groups were co-cultured with human CD8+ T cells respectively. *$p < 0.05$, **$p < 0.01$, ***$p < 0.001$.

in cells with *SRD5A3* knockdown was significantly increased (Figure 9C). Transwell experiments showed that compared with the control group si-NC, the migration and invasion abilities of cells in the si-SRD5A3 group were significantly reduced (Figure 9D,E). HepG2 cell lines and knockdown cell lines were co-cultured with human CD8+ T cells respectively. ELISA detected the expression levels of IFN-γ, CD27, and CD28 in cells, and found that the expression levels of IFN-γ, CD27, and CD28 in the knockdown cell line group were significantly higher than those in the control group (Figure 9F).

4. Discussion

The pathogenesis of LIHC involves joint regulation of multiple factors such as the environment, genetic variation, and multiple signaling pathways [21]. The disease is difficult to detect in the early stages, but it progresses rapidly and the mortality rate increases annually. Hence, the research on early diagnostic markers and molecular targets is urgent [22,23]. In recent years, studies on TME have found that non-tumor components play important roles in the occurrence and development of cancer [24,25]. The immune matrix components in the TME change dynamically. These subtle changes often indicate different responses of patients to anti-cancer treatment and drug resistance, and are positively related to the prognosis of patients with tumor [26,27].

Steroid hormones are essential for stress response, immune system regulation and reproduction in mammals. Testosterone or progesterone is catalyzed by the *SRD5As* to produce the corresponding steroid, which is essential for a variety of physiological and pathological processes. As a protein-coding gene, *SRD5A3* is a member of the *SRD5A* family and plays a regulatory role in human development and the production of steroid hormones by catalyzing the conversion of testosterone into the most potent natural androgen. In this study, the survival rate of patients with *SRD5A3*-expressing LIHC was found to be significantly poorer in patients with LIHC with upregulated *SRD5A3*, which was related to the grade or stage of the tumor. By screening the differentially expressed genes, further enrichment analysis showed that they were enriched in the biological processes of immune cell responses and matrix interactions. *SRD5A3* is mainly involved in processes such as immune cells and immune responses in TME. The reduced immune infiltration levels of CD8+ T, CD4+ T, and B cells in patients with LIHC are associated with the increased expression of *SRD5A3*. Decrease in the expression levels of CD27 and CD28 was closely related to *SRD5A3* overexpression. Clinical specimens have verified that *SRD5A3* is highly expressed in liver cancer tissues. The expression of *SRD5A3* in liver cancer cell lines is higher than that in normal liver cell lines. *In vitro* experiments have proven that increased expression of *SRD5A3* leads to the proliferation and metastasis of liver cancer cell lines, and knockdown of liver cancer cell lines can inhibit this phenomenon. In addition, the ability of co-cultured CD8+ T cells to express IFN-γ, CD27, and CD28 is obviously related to the expression of *SRD5A3*. The stronger the expression ability of *SRD5A3* in liver cancer cell lines, the weaker the expression ability of CD8+ T cells.

CD27, a member of the tumor necrosis factor (TNF) receptor superfamily, is expressed in most immune cells [28,29]. Transmembrane phosphoglycoproteins are mainly expressed in CD4+ and CD8+ T cells [30]. Its expression increases during T-cell activation and is shed from the cell surface, where it can form soluble CD27 (sCD27) upon activation. After binding to CD70, CD27 generates intracellular signals that enhance the activation of T, B, and natural killer (NK) cells [31]. CD27–CD70 signaling has also been reported to further promote B-cell activation and plasma cell differentiation, increase cytotoxic CD8+ T cell activity, promote T-cell production of TNF-α, and increase NK cell activity through the production of interferon gamma (IFN-γ) and interleukin factors [32]. Currently, all CD27-targeting antibodies in clinical stages are agonist antibodies. They have been extensively studied *in vitro* and *in vivo* in clinical trials across a range of hematological and solid tumor types [33,34].

As the first costimulatory receptor discovered, CD28 is the founding member of a subfamily of costimulatory molecules characterized by extracellular variant immunoglobulin-like domains [35]. CD28 mainly serves as a 'second signal' to lower the threshold required to effectively activate T cells, and strengthens the 'first signal' to activate T cells, allowing them to further develop and proliferate into cells with immune functions [36,37]. In addition, CD28 and the co-inhibitory receptor CTLA-4, together with their shared ligands B7-1 and B7-2, constitute the best-characterized regulatory T-cell pathways and are examples of other co-stimulatory and co-inhibitory pathways [38]. The interaction between CD28 and CTLA-4 is crucial for immune activation or suppression during the development of CD28-targeted modulators [39–42]. Simultaneously, it reduces the risk of cytokine storms caused by the strong T-cell activation ability of CD28 activators [43].

Under TME, a variety of immune cells interact with tumor cells to regulate tumor growth and respond to tumor treatments such as targeted drugs. These results indicate that the TME is closely related to tumor growth, and an in-depth research on its related genes is of great significance. The standards explored in this study were based on the relevant verification of objective bioinformatics indicators and experimental data. These indicators may be more conducive for the detection of immune checkpoint inhibitors commonly used in clinical practice. However, this study has some limitations. Although high immune prediction efficacy was observed in the dataset, we were unable to obtain an immunotherapy-related cohort to verify the utility of this study. Furthermore, converting these goals into

clinical decisions remains challenging. The mechanisms involved need to be further verified by *in vivo* and *in vitro* experiments.

5. Conclusions

This study analyzed the single-cell sequencing data of LIHC samples in a database based on bioinformatics methods and *in vitro* experiments, and found that high expression of SRD5A3 was significantly associated with poor prognosis in patients with LIHC. Moreover, high SRD5A3 expression may lead to poor tumor immune infiltration and promote the migration, invasion, and proliferation of liver cancer cells, thereby affecting the efficacy of immunotherapy. This discovery holds promise for the further exploration of suitable immunotherapeutic targets. Therefore, this gene can be used as a biomarker to judge the prognosis of patients with LIHC and has reference significance for the selection of clinical treatment options.

Authors contributions

Research idea: YML, WDL, YZ. Data extraction and integrated analysis: YML, WDL, YZ, ZWL, XSL, XQL. Quality assessment and result interpretation: YML, WDL, YZ, ZWL, XSL, XQL, KM, NGC. Modification and polishing: KM and NGC. Manuscript writing: All authors. Final approval of manuscript: All authors. Agree to be accountable for all aspects of the work: All authors.

Ethics approval and consent to participate

This study was conducted under the approval of the Ethics Committee of the Shen Shan Medical Center, Memorial Hospital of Sun Yat-Sen University in strict accordance with the Declaration of Helsinki. No animal studies, human studies in this manuscript. I confirm that all the research meets ethical guidelines and adheres to the legal requirements of the study country. All patients were informed prior to use of patient specimen and signed written informed consents.

Disclosure statement

The authors declare that the research was conducted in the absence of any commercial or financial relationships that could be construed as a potential conflict of interest.

Funding

This research was supported by the Scientific research project of Guangdong Provincial Bureau of Traditional Chinese Medicine (20231419).

ORCID

Yuming Lu http://orcid.org/0009-0007-6527-0465
Weida Lin http://orcid.org/0009-0002-3827-013X

Data availability statement

The original contributions presented in the study are included in the article, further inquiries can be directed to the corresponding authors.

References

[1] Cheng K, Cai N, Zhu J, et al. Tumor-associated macrophages in liver cancer: from mechanisms to therapy. Cancer Commun (Lond). 2022;42(11):1112–1140. doi: 10.1002/cac2.12345.
[2] Li X, Ramadori P, Pfister D, et al. The immunological and metabolic landscape in primary and metastatic liver cancer. Nat Rev Cancer. 2021;21(9):541–557. doi: 10.1038/s41568-021-00383-9.
[3] Anwanwan D, Singh SK, Singh S, et al. Challenges in liver cancer and possible treatment approaches. Biochim Biophys Acta Rev Cancer. 2020;1873(1):188314. doi: 10.1016/j.bbcan.2019.188314.
[4] Xu F, Jin T, Zhu Y, et al. Immune checkpoint therapy in liver cancer. J Exp Clin Cancer Res. 2018;37(1):110. doi: 10.1186/s13046-018-0777-4.
[5] Llovet JM, Kelley RK, Villanueva A, et al. Hepatocellular carcinoma. Nat Rev Dis Primers. 2021;7(1):6. doi: 10.1038/s41572-020-00240-3.
[6] Forner A, Reig M, Bruix J. Hepatocellular carcinoma. Lancet. 2018;391(10127):1301–1314. doi: 10.1016/S0140-6736(18)30010-2.
[7] Xue R, Zhang Q, Cao Q, et al. Liver tumour immune microenvironment subtypes and neutrophil heterogeneity. Nature. 2022;612(7938):141–147. doi: 10.1038/s41586-022-05400-x.
[8] Donne R, Lujambio A. The liver cancer immune microenvironment: therapeutic implications for hepatocellular carcinoma. Hepatology. 2023;77(5):1773–1796. doi: 10.1002/hep.32740.
[9] Stiles AR, Russell DW. SRD5A3: a surprising role in glycosylation. Cell. 2010;142(2):196–198. doi: 10.1016/j.cell.2010.07.003.
[10] Chávez B, Ramos L, García-Becerra R, et al. Hamster SRD5A3 lacks steroid 5α-reductase activity in vitro. Steroids. 2015;94:41–50. doi: 10.1016/j.steroids.2014.11.005.
[11] Wang ZH, Zhang YZ, Wang YS, et al. Identification of novel cell glycolysis related gene signature predicting survival in patients with endometrial cancer. Cancer Cell Int. 2019;19(1):296. doi: 10.1186/s12935-019-1001-0.
[12] O'Shaughnessy PJ, Monteiro A, Bhattacharya S, et al. Steroidogenic enzyme expression in the human fetal liver and potential role in the endocrinology of pregnancy. Mol Hum Reprod. 2013;19(3):177–187. doi: 10.1093/molehr/gas059.
[13] Zhang YP, Na WT, Dai XQ, et al. Over-expression of SRD5A3 and its prognostic significance in breast cancer. World J Surg Oncol. 2021;19(1):260. doi: 10.1186/s12957-021-02377-1.

[14] Han Y, Wang Y, Dong X, et al. TISCH2: expanded datasets and new tools for single-cell transcriptome analyses of the tumor microenvironment. Nucleic Acids Res. 2023;51(D1):D1425–d1431. doi: 10.1093/nar/gkac959.
[15] Liu J, Lichtenberg T, Hoadley KA, et al. An integrated TCGA pan-cancer clinical data resource to drive high-quality survival outcome analytics. Cell. 2018;173(2):400–416.e411. doi: 10.1016/j.cell.2018.02.052.
[16] Barrett T, Wilhite SE, Ledoux P, et al. NCBI GEO: archive for functional genomics data sets–update. Nucleic Acids Res. 2013;41(Database issue):D991–995. doi: 10.1093/nar/gks1193.
[17] Gene ontology consortium: going forward. Nucleic Acids Res. 2015;43(Database issue):D1049–1056.
[18] Kanehisa M, Furumichi M, Tanabe M, et al. KEGG: new perspectives on genomes, pathways, diseases and drugs. Nucleic Acids Res. 2017;45(D1):D353–d361. doi: 10.1093/nar/gkw1092.
[19] Li T, Fan J, Wang B, et al. TIMER: a web server for comprehensive analysis of tumor-infiltrating immune cells. Cancer Res. 2017;77(21):e108–e110. doi: 10.1158/0008-5472.CAN-17-0307.
[20] Szklarczyk D, Gable AL, Nastou KC, et al. The STRING database in 2021: customizable protein-protein networks, and functional characterization of user-uploaded gene/measurement sets. Nucleic Acids Res. 2021;49(D1):D605–d612. doi: 10.1093/nar/gkaa1074.
[21] Wang G, Wang Q, Liang N, et al. Oncogenic driver genes and tumor microenvironment determine the type of liver cancer. Cell Death Dis. 2020;11(5):313. doi: 10.1038/s41419-020-2509-x.
[22] Wei C-Y, Zhu M-X, Zhang P-F, et al. PKCα/ZFP64/CSF1 axis resets the tumor microenvironment and fuels anti-PD1 resistance in hepatocellular carcinoma. J Hepatol. 2022;77(1):163–176. doi: 10.1016/j.jhep.2022.02.019.
[23] Wang H, Lu Z, Zhao X. Tumorigenesis, diagnosis, and therapeutic potential of exosomes in liver cancer. J Hematol Oncol. 2019;12(1):133. doi: 10.1186/s13045-019-0806-6.
[24] Massalha H, Bahar Halpern K, Abu-Gazala S, et al. A single cell atlas of the human liver tumor microenvironment. Mol Syst Biol. 2020;16(12):e9682. doi: 10.15252/msb.20209682.
[25] Huang Y, Wang S, Ke A, et al. Ferroptosis and its interaction with tumor immune microenvironment in liver cancer. Biochim Biophys Acta Rev Cancer. 2023;1878(1):188848. doi: 10.1016/j.bbcan.2022.188848.
[26] Ma L, Heinrich S, Wang L, et al. Multiregional single-cell dissection of tumor and immune cells reveals stable lock-and-key features in liver cancer. Nat Commun. 2022;13(1):7533. doi: 10.1038/s41467-022-35291-5.
[27] Affo S, Yu LX, Schwabe RF. The role of cancer-associated fibroblasts and fibrosis in liver cancer. Annu Rev Pathol. 2017;12(1):153–186. doi: 10.1146/annurev-pathol-052016-100322.
[28] Buchan SL, Rogel A, Al-Shamkhani A. The immunobiology of CD27 and OX40 and their potential as targets for cancer immunotherapy. Blood. 2018;131(1):39–48. doi: 10.1182/blood-2017-07-741025.
[29] Starzer AM, Berghoff AS. New emerging targets in cancer immunotherapy: CD27 (TNFRSF7). ESMO Open. 2020;4(Suppl 3):e000629. doi: 10.1136/esmoopen-2019-000629.
[30] Claus C, Riether C, Schürch C, et al. CD27 signaling increases the frequency of regulatory T cells and promotes tumor growth. Cancer Res. 2012;72(14):3664–3676. doi: 10.1158/0008-5472.CAN-11-2791.
[31] Gong L, Luo J, Zhang Y, et al. Nasopharyngeal carcinoma cells promote regulatory T cell development and suppressive activity via CD70-CD27 interaction. Nat Commun. 2023;14(1):1912. doi: 10.1038/s41467-023-37614-6.
[32] Benhamouda N, Sam I, Epaillard N, et al. Plasma CD27, a surrogate of the intratumoral CD27-CD70 interaction, correlates with immunotherapy resistance in renal cell carcinoma. Clin Cancer Res. 2022;28(22):4983–4994. doi: 10.1158/1078-0432.CCR-22-0905.
[33] Turaj AH, Hussain K, Cox KL, et al. Antibody tumor targeting is enhanced by CD27 agonists through myeloid recruitment. Cancer Cell. 2017;32(6):777–791.e776. doi: 10.1016/j.ccell.2017.11.001.
[34] Wajant H. Therapeutic targeting of CD70 and CD27. Expert Opin Ther Targets. 2016;20(8):959–973. doi: 10.1517/14728222.2016.1158812.
[35] Waite JC, Wang B, Haber L, et al. Tumor-targeted CD28 bispecific antibodies enhance the antitumor efficacy of PD-1 immunotherapy. Sci Transl Med. 2020;12(549):eaba2325. doi: 10.1126/scitranslmed.aba2325.
[36] Banta KL, Xu X, Chitre AS, et al. Mechanistic convergence of the TIGIT and PD-1 inhibitory pathways necessitates co-blockade to optimize anti-tumor CD8(+) T cell responses. Immunity. 2022;55(3):512–526.e519. doi: 10.1016/j.immuni.2022.02.005.
[37] Huff WX, Kwon JH, Henriquez M, et al. The evolving role of CD8(+)CD28(-) immunosenescent t cells in cancer immunology. Int J Mol Sci. 2019;20(11):2810. doi: 10.3390/ijms20112810.
[38] Kamphorst AO, Wieland A, Nasti T, et al. Rescue of exhausted CD8 T cells by PD-1-targeted therapies is CD28-dependent. Science. 2017;355(6332):1423–1427. doi: 10.1126/science.aaf0683.
[39] Cappell KM, Kochenderfer JN. A comparison of chimeric antigen receptors containing CD28 versus 4-1BB costimulatory domains. Nat Rev Clin Oncol. 2021;18(11):715–727. doi: 10.1038/s41571-021-00530-z.
[40] Hui E, Cheung J, Zhu J, et al. T cell costimulatory receptor CD28 is a primary target for PD-1-mediated inhibition. Science. 2017;355(6332):1428–1433. doi: 10.1126/science.aaf1292.
[41] Duraiswamy J, Turrini R, Minasyan A, et al. Myeloid antigen-presenting cell niches sustain antitumor T cells and license PD-1 blockade via CD28 costimulation. Cancer Cell. 2021;39(12):1623–1642.e1620. doi: 10.1016/j.ccell.2021.10.008.
[42] Rowshanravan B, Halliday N, Sansom DM. CTLA-4: a moving target in immunotherapy. Blood. 2018;131(1):58–67. doi: 10.1182/blood-2017-06-741033.
[43] Zappasodi R, Serganova I, Cohen IJ, et al. CTLA-4 blockade drives loss of T(reg) stability in glycolysis-low tumours. Nature. 2021;591(7851):652–658. doi: 10.1038/s41586-021-03326-4.